Centre for Applied Energy Economics & Policy Research: Working Paper Series 2022-06

Griffith UNIVERSITY
Griffith Business School
Queensland, Australia

Quantifying the risk of renewable energy droughts in Australia's National Electricity Market (NEM) using MERRA-2 weather data

Joel Gilmore, Tim Nelson, and Tahlia Nolan[§]
Griffith University
Nathan, QLD 4111

July 2022

It is anticipated that Australia's National Electricity Market (NEM) will be almost entirely dependent upon variable renewable energy (VRE) production in the coming decades. The Australian Energy Market Operator (AEMO) and other researchers have provided detailed forecasts of the storage and firming required to ensure a secure electricity system that is supplied exclusively by VRE. However, these forecasts utilise existing VRE datasets which are often limited by historical observation given the relatively recent deployment of renewables in the Australian electricity system. This article seeks to significantly expand this analysis by building a VRE output forecast model that utilises 42 years of real-world weather data. This 'backcasting' approach allows us to far more accurately determine firming and storage requirements to overcome real-world instantaneous and medium-term production risk in a system supplied entirely by VRE resources. Our results can be used by policy makers to better plan the just transition to a renewable energy-based electricity system.

Keywords: renewable energy; electricity markets; energy market modelling

JEL Codes: Q41; Q47; D47

[§] Joel Gilmore is an Associate Professor at Centre for Applied Energy Economics & Policy Research, Griffith University. Tim Nelson is an Associate Professor at Griffith University. Tahlia Nolan is PhD candidate at Griffith University. All views, errors and omissions are entirely the responsibility of the authors, not Griffith. Correspondence to joel.gilmore@griffith.edu.au.

Centre for Applied Energy Economics and Policy Research

1. Introduction

Through the United Nations Framework Convention on Climate Change (UNFCCC) process, Australia has committed to reducing its greenhouse gas emissions in a manner that limits anthropogenic climate change to no more than 2 degrees Celsius with an aspiration to achieve no more than 1.5 degrees. Meinshausen et al., 2022 estimate that this commitment will require Australian emission reductions of ~50 to ~75% by 2030. Given that the electricity sector is currently the source of around one-third of Australia's annual emissions due to its heavy reliance upon coal, it is highly likely that addressing climate change will involve complete decarbonisation of the Australian electricity system by the early 2030s (see Gilmore et al, 2022).

Australian policy makers have determined that decarbonisation of the electricity sector will be achieved through the utilisation of renewable energy. State governments have established significant policies to support investment in onshore and offshore renewable energy and associated transmission infrastructure (Nelson et al., 2022). The Australian Market Operator (AEMO) produces a blueprint for this sector transition known as the Integrated System Plan (ISP). Through detailed system modelling, the ISP projects the required energy storage (i.e. batteries and pumped hydro) and firming (i.e. peaking plant) required to give effect to a system dependent upon variable solar and wind resources.

A critical and underexplored policy issue in the Australian context is the potential for 'energy droughts' (often referred to as "dunkelflaute" periods) to exhaust energy storage and leave the electricity system vulnerable to supply interruptions. While the market operator and other researchers have used existing solar and wind output traces to optimise the projected storage and firming technologies to address these 'energy droughts', the relatively recent emergence of solar and wind technologies may mean that data sets are simply not long dated enough to provide sufficient guidance for policy makers.

Data on potential solar and wind output does exist though in the form of longer-term weather datasets. With appropriate analysis, it is possible to utilise these long-term weather datasets to simulate how much energy would have been captured historically if solar and wind energy production technologies had been in place. In this paper, we utilise this method to provide a much longer dated dataset of historical wind and solar output across Australia. This analysis provides us with significant insights into VRE output variability and in particular, answers to two important questions for policy makers:

- *Instantaneous production risk and the optimal level of firming capacity* – what is the probability distribution of the lowest VRE output expected at any time? When correlated with projected electricity demand and coupled with an appropriate reliability standard, we can determine the capacity (in MW) of firming capacity required. For example, could there be a scenario where there is *zero* instantaneous wind and solar production and all energy production will need to be sourced from batteries, pumped hydro or other firming technologies?

- *The potential for VRE 'droughts' and implications for energy storage* - what is the probability distribution of total energy provided over a given interval (e.g., across an hour, a day, or a week)? In a 100% VRE system, understanding the extent of energy 'droughts' and 'floods' determines the quantity of storage (in MWh) required, and

over what timeframe– sufficient to smooth out the available energy across an hour, day, week, season, etc.

Importantly, it is the statistical 'long-tail' of low production periods that will determine firming requirements. Utilising longer dated datasets to produce more detailed analysis of energy flows in a future VRE based electricity system will allow policy makers to better understand the trade-off between cost and reliability. The purpose of this article is to significantly expand policy makers understanding of these issues by utilising this hitherto underexplored technique in the Australian context. Our review of the literature is presented in Section 2. The methodology and data used in our analysis is outlined in Section 3. Section 4 catalogues our results and Section 5 provides detailed discussion and our policy recommendations and concluding remarks.

2. Literature Review

Understanding the potential variability of VRE resource requires a long time series, statistical models, or both. The simplest option is to use historical production data from actual projects. However, such data only goes back as far as projects exist and will not necessarily reflect future geographical distributions or diversity of projects. It can also be difficult to separate[1] the underlying weather resource from changes in technology (e.g., panel or turbine efficiency), network constraints and grid outages (Staffell and Green, 2014). The second option is collating historical ground-based weather station observations (for example, (Katsigiannis and Stavrakakis, 2014; Sinden, 2007)). Importantly, this can provide a timeseries for as long as measurements were taken. Limitations of this approach can include data not typically being available at locations representative of wind farms and scaling the observations to windfarm hub height.

The third option is a combination of the two approaches through reanalysis - backcasting historical weather conditions by calibrating atmospherical weather models to observed historical observations (Ebisuzaki and Zhang, 2014). Data sources include measurements from satellites, ground-based weather stations, and other sources. The end goal is a consistent weather dataset with much higher spatial resolution than can be obtained from only physical historical measurements. This makes reanalyses ideal for assessing the variability around renewable energy resources over long time periods. One such dataset is the NASA Modern-Era Retrospective Analysis for Research and Applications, Version 2 (MERRA-2) reanalysis (Gelaro et al., 2017) which provides global coverage at 0.5 x 0.625 degree resolution (roughly 50 km x 50 km in Australia) from 1980 to the present.

Across several key papers, Staffell, Green,and Pfenningerhave developed methods for simulating wind and solar traces based on the MERRA-2 dataset. In two of these papers (Staffell and Green, 2014; Staffell and Pfenninger, 2016) the authors developed a Virtual Wind Farm model benchmarked against existing wind farms. Wind speed data was extracted from the MERRA-2 data set and extrapolated to hub height and run through a simulated

[1] Transmission constraints, grid and plant outages, maintenance, and commissioning delays are all important issues, but can and should be considered separately to the underlying resource drought.

power curve, with appropriate adjustments for wind variability across a farm[2]. They also developed a procedure for adjusting biases in the MERRA-2 dataset for each country to match metered generation data, which allows for some adjustment to reflect mesoscale trends. Pfenninger and Staffell (2016) used a similar approach for solar power, including correcting biases in solar data by calibrating to 1000 solar sites across Europe. This allowed for insightful analysis of the variability in solar output across hours and days.

This approach has been used in other works. McPherson et al., (2017) developed a similar tool for forecasting wind and solar generation, and then used these traces to simulate future grid scenarios for Canada (McPherson and Karney, 2017). Ofgem, (2012) undertook an assessment of capacity adequacy in the UK including simulation of UK wind farms using the original MERRA dataset. They present backcast simulations of wind production against metered data, concluding accuracy was high enough for the purpose of statistical wind distributions using 32 years of simulated wind data. Wind power has been modelled in Sweden by Olauson and Bergkvist (2016), who developed country-based time series of wind power output across Europe. They found correlations between projects decline exponentially with distance and are highest for long-term (greater than four months) trends and lowest for step change and short-term features.

Reanalysis data sets are increasingly being used to investigate long-term firming requirements and the ability to deliver 100% renewable systems. Tong et al., (2021) used the MERRA-2 dataset to simulate high VRE systems across 42 countries, identifying resource adequacy with different combinations and levels of renewable energy resource. Poletti and Staffell (2021) utilised MERRA-2 data to demonstrate resource adequacy of a 100% renewable electricity New Zealand grid with 7-day storage.

William et al. (2019) used a long-term reanalysis weather dataset to model 100% renewables in Europe by 2050, based on 37 years of reference data. They found that similar levels of reliability to today could be achieved, but would require significant transmission augmentation to benefit from geographic resource diversity. Ohlendorf and Schill (2020) used MERRA-2 data to evaluate low-wind-power events, and found a one-in-ten year event would be wind operating at less than 10% average capacity factor for nearly eight days.

Despite global usage, application and verification of MERRA, MERRA-2, or other reanalysis datasets in Australia have been limited. Hallgren et al. (2014) developed a wind map for Australia, based on MERRA wind speeds, but did not seek to simulate or benchmark existing wind farms. Wang et al. (2018) used MERRA-2 data for some traces, but only for a single reference year. Prasad et al. (2017) investigated the correlation of wind and solar resources across Australia, and found resources could be complementary, particularly if

[2] Care must be taken to use an appropriate power curve. A manufacturer's turbine curve may appropriate for a single wind turbine, but does not adequately describe the output of a farm with multiple turbines once spatial and temporal variation in wind speeds is taken into account. Nørgaard and Holttinen (2004) presented a possible solution where a single-turbine power curve is convoluted with a probability distribution (normal or otherwise) of wind speeds. They found this to be highly effective, and it has been widely adopted, including in the Python windpowerlib library used in this article.

separated by 500km or more. This paper therefore provides a calibration and validation of the MERRA-2 data to Australian conditions.

One potential risk that cannot be captured through historical reanalysis is that historical patterns will change in more extreme climate change scenarios. Wild et al., (2015) analysed projections from 39 climate models from the Coupled Model Intercomparison Project Phase 5 (CMIP5), and observed material decreases (over 1%/decade) in solar photovoltaic (PV) output from 2006 to 2049 in higher heating scenarios. Long-term wind studies are more mixed, with shifting patterns of wind power (Santos et al., 2015).

3. Methodology and Data

3.1 MERRA-2 data

MERRA-2 data was downloaded for the period 1st Jan 1980 to 31st December 2021 from the NASA Goddard Earth Sciences Data and Information Services Centre. Hourly, time-averaged data was extracted for each grid point (Figure 1) and compiled into a local database suitable for extracting specific sites.

Figure 1 MERRA-2 grid points for east coast of Australia[3]

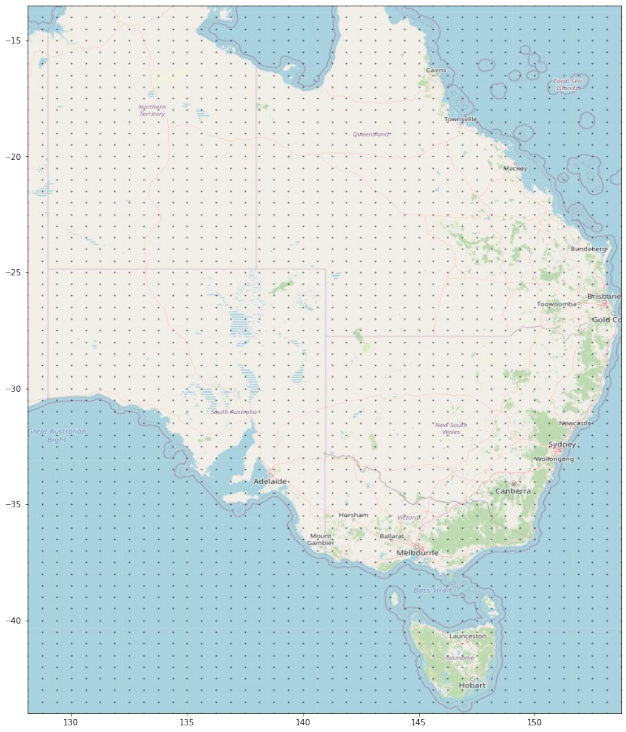

[3] Map figure from Open Street Maps

3.2 Wind modelling

Wind production was modelled using the open source Python package *windpowerlib* (Haas et al., 2021), which implements useful algorithms for extrapolating from the MERRA-2 data including a logarithmic scaling of wind speeds from measured levels (2m, 10m, and 80m) to hub height, spatial smoothing of wind speeds across a farm following the approach of Staffell and Pfenninger (2016), and a model of wake losses by Kohler et al. (2010). Details were compiled for each existing wind farm in the NEM. Where data was available, the manufacturer reported power curve (mapping of wind speed to MW output of the turbine) of the wind farm was used; otherwise, the power curve of a similar sized turbine was used.

The raw MERRA-2 wind data produced high quality outputs at the regional (aggregate) level, with both qualitative (correlations, generation-duration curve trends, etc) and quantitative (capacity factors) features aligning well with historical data. However, the projected capacity factor for any individual wind projects was sometimes much higher or much lower than observed. Raw wind speeds w for each site were scaled and offset through the general form

$$w' = \alpha \cdot w + \beta$$

where suitable α and β parameters were determined for each individual wind farm to best match the historical generation-duration curve. β was iteratively adjusted until the target capacity factor was achieved, then α adjusted to better match the P20 and P80 (20% and 80% probability of exceedance) production[4], and the process iterated to best match. As part of the calibration and benchmarking, obvious periods of network or economic constraints and forced or planned outages were corrected for but an exhaustive search of all periods was not undertaken. A 3% derating to all individual backcast traces was assumed to capture the average impact of lost production. This process was undertaken for three calendar years (Cal19 to Cal21) and was reasonably consistent between years. To avoid overfitting, the benchmarked α and β were averaged across the three years for each site and applied to all years. This produced high quality projections for each site (for example, Figure 2 showing the Taralga wind farm), which was used for the *Existing Fleet* backcast.

[4] For example, if the 20% POE backcast was higher than actuals, α would be lowered (reducing high demand periods more than low) and then β increased to return to the same capacity factor.

Figure 2 Example of backcast wind output for one wind farm (Taralga, July-August 2020)

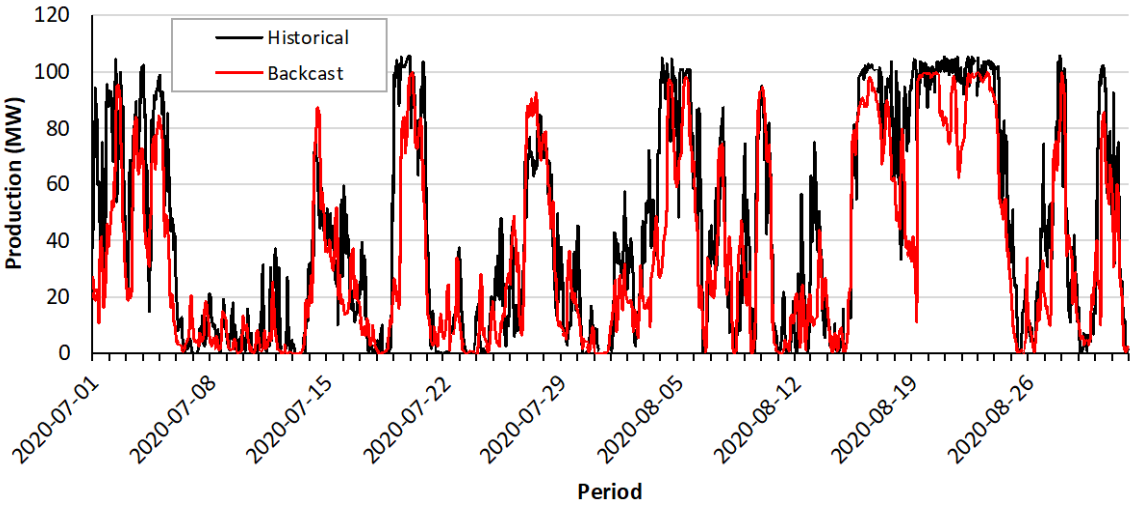

To select appropriate α and β for *new* sites in a future NEM mainland fleet, a regional calibration factor for each of the mainland states (combining Queensland with New South Wales, due to lack of data in Queensland) was determined by simulating all sites for which historical data was available and targeting the regional generation-duration curve. In general, relatively little scaling was required at the regional level (with wind traces scaled by up to 12% and adjusted by between -0.5m/s and 0.08m/s). This is consistent with the expectation that local factors can either positively or negatively impact the MERRA-2 wind traces, and are averaged out across enough sites. In South Australia, subsequent simulation of wind farms with modern turbines yielded very high capacity factors (>50%) which does not match recent experience and a 5% wind speed reduction was manually applied. Finally, a further 5% wind speed reduction was applied to all sites to reflect a likely reduction in the availability of high-quality development sites with significant new build.

When applied to the existing fleet, this approach delivered a close match on daily, weekly and hourly resolutions as shown by the figures below. Critically, performance during low wind conditions matched well over various timescales, which is important for analysis of potential VRE droughts.

Figure 3 NEM Wind average daily production, historical and backcast for Cal19-Cal21

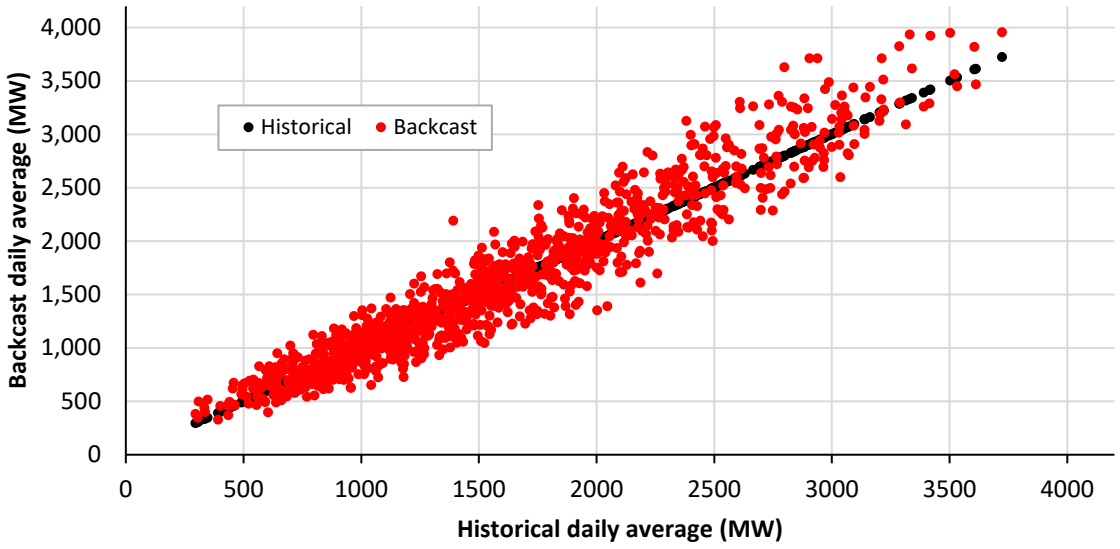

Figure 4 NEM Wind average weekly production, historical and backcast for Cal20[5]

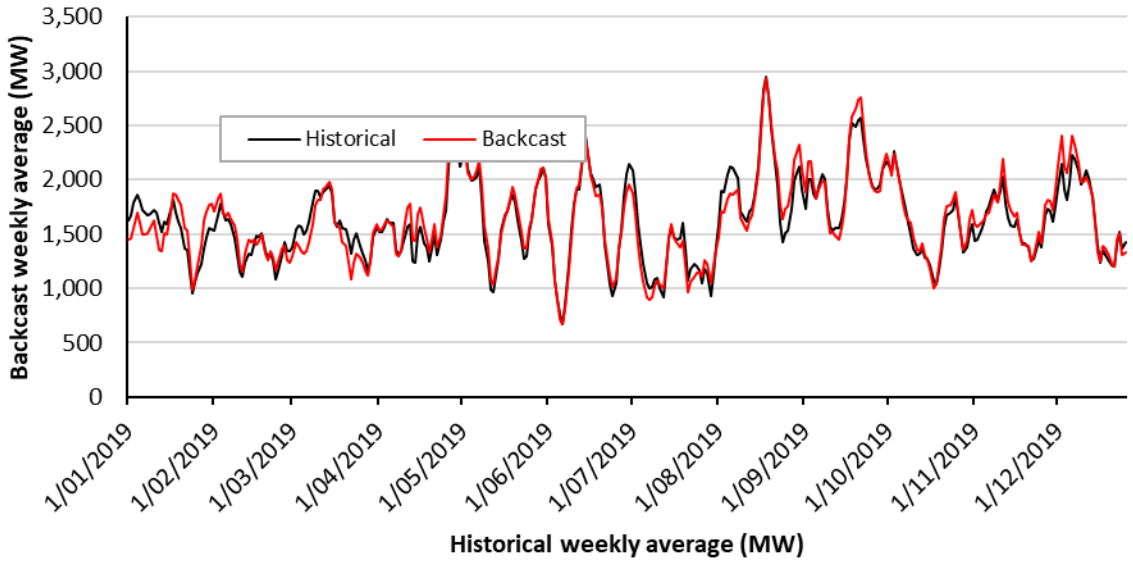

[5] Cal20 shown instead of Cal21 due to transmission constraints in the historical dataset in Cal21

Figure 5 NEM Wind production duration curve, historical and backcast using regional calibration factors for Cal20[6]

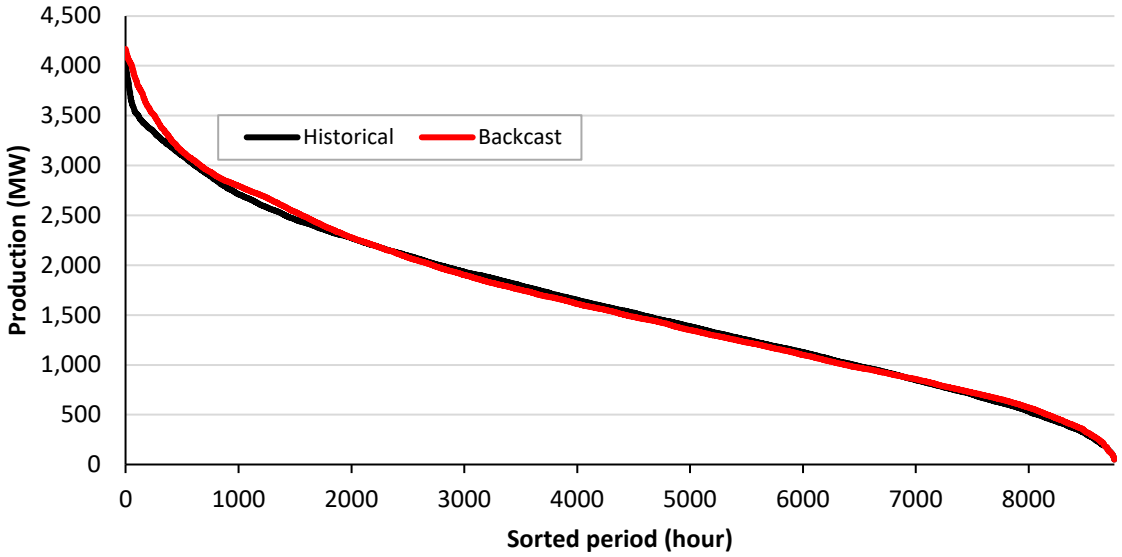

Figure 6 NEM Wind example hourly production, historical and backcast (July-August 2020)

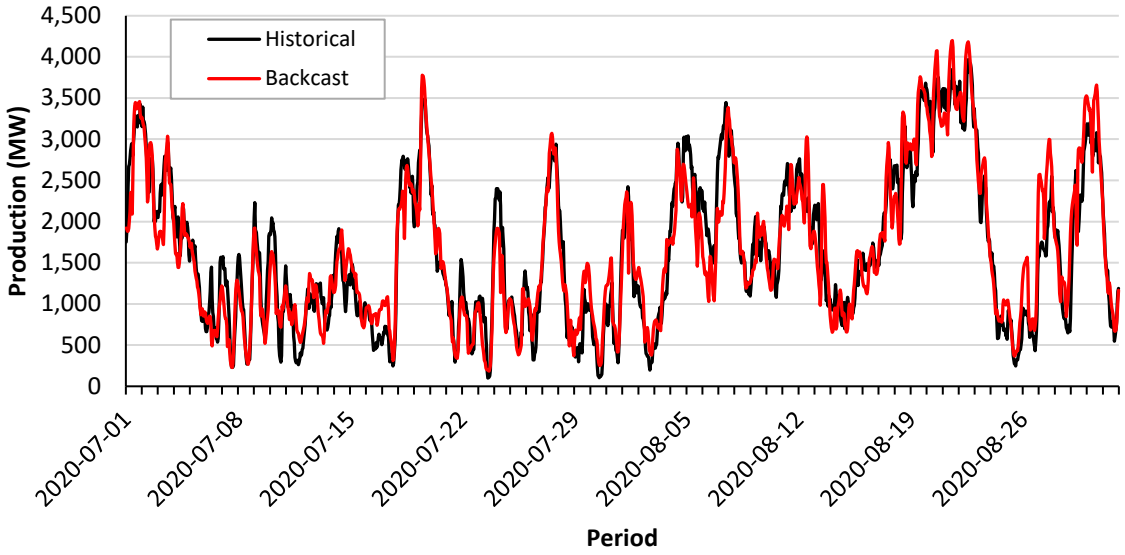

[6] Cal20 shown instead of Cal21 due to transmission constraints in the historical dataset in Cal21

3.3 Large-scale solar

The open source package pvlib (Holmgren et al., 2018) was used to simulate large-scale solar projects. The MERRA-2 dataset provides Global Horizonal Insolation (GHI; the total solar radiation incident on a horizontal plane) for each location but not Direct Normal Insolation (DNI; solar radiation on a plane directly facing the sun) which is required for simulating solar systems with tracking. Many methods have been proposed to estimate the DNI from observed GHI, the location of the sun based on physics models, and an atmospheric model; we used the DISC algorithm (Maxwell, 1987), implemented by pvlib[7].

For benchmarking against existing projects, both transmission and economic constraints occurred regularly for solar PV. These periods were filtered where possible through constraining the simulations to historical maximum MW constraints[8], or excluding sites with significant curtailment. As with wind projects, a 3% average derating was applied to all traces to capture forced and unforced outages.

Figure 7 and Figure 8 show the historical and backcast output of 15 solar projects totalling 1053 MW across the New South Wales, Victoria, and South Australian regions of Australia over calendar year 2021. The MERRA-2 dataset produces very high correlation at a daily (correlation factor=0.959) and weekly (correlation factor=0.980) averaged resolution, suggesting this is a suitable dataset for understanding the role of droughts and long-duration storage[9].

[7] The pvlib implementation appears to assume all input values refer to instantaneous measurements . Due to the use of *average* hourly MERRA-2 data, providing inputs “on the hour” resulted in unrealistic outputs if input *average* GHI was higher than the theoretical *instantaneous* clear-sky GHI. Effective results were obtained for the Australian east coast by casting inputs as being measured at 40 minutes past the hour.

[8] Any daytime periods with historical production less than 5% of nameplate were assumed to be curtailed periods, and were set to the same level in the backcast.

[9] Correlation at hourly resolution is also very high (0.981) but this metric is confounded by the intrinsic diurnal nature of solar.

Figure 7 NSW Solar daily average MW, actuals vs backcast for Cal21

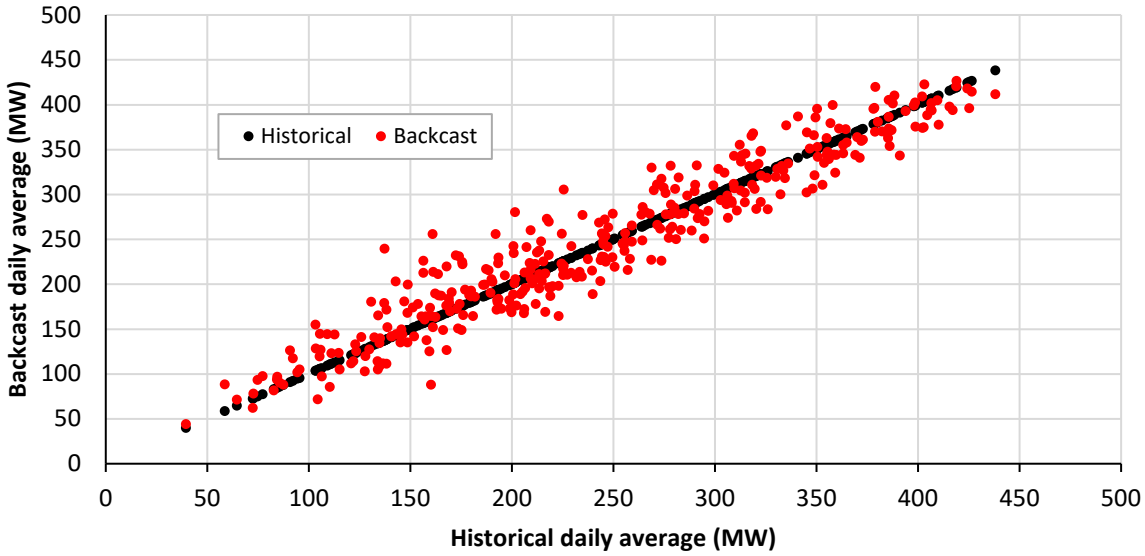

Figure 8 NSW Solar weekly average MW, actuals and backcast for Cal21

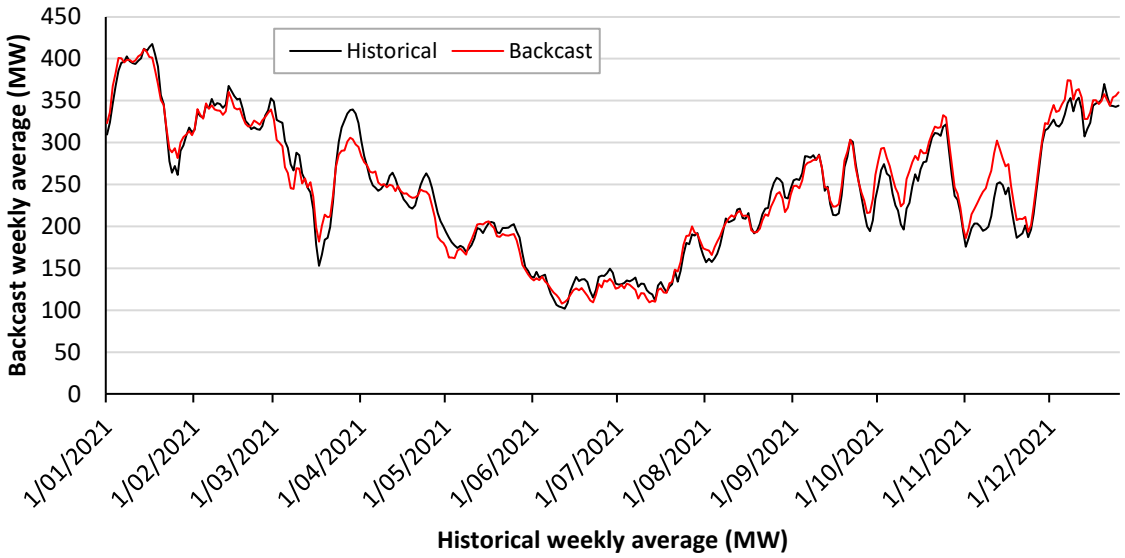

3.4 Rooftop PV

Rooftop PV statistics including the installed capacity by system size, number of systems by system size, and number of dwellings were downloaded from the Australian PV Institute

(APVI) Solar Map site[10] for each State Electoral Division (SED) geographical region. No comprehensive data was available as to the distribution of system configurations, so assumptions were tested and refined against subsequent benchmarking. Simulations for each location were distributed between North, East, and West facing, set at an angle of 20 degrees consistent with roof pitches in Australia of 15 to 22.5 degrees. AC and DC capacities were matched.

Given the resolution of the MERRA-2 grid points, 116 distinct locations were simulated across 326 SEDs. Regional rooftop PV backcasts were calibrated against regional half-hourly rooftop PV production estimates provided by AEMO. The historically installed rooftop PV capacity at monthly resolution was used to scale the simulated historical rooftop PV traces (the share of dwellings with rooftop PV by SED was held constant at December 2021 levels). Based on an initial comparison, the simulated rooftop PV traces were scaled by 0.728 to 0.755 (depending on the region) to match the historically reported annual capacity factor, which captures the lower performance of distributed rooftop systems compared to well-maintained utility scale projects. It was also observed that particularly low generation days (less than 65-80% of expected clear sky conditions output) were overestimated in the backcast, and so a further 15-30% derating was applied to all output in that region on those days. Figure 9 shows the daily and diurnal average output of the MERRA-2 model (red) versus the AEMO reported data (black). The hourly generation-duration curve and monthly average generation curves also matched closely.

Figure 9 Rooftop PV backcast of average daily mean MW (left) and average diurnal mean MW (right) (2019-2021)

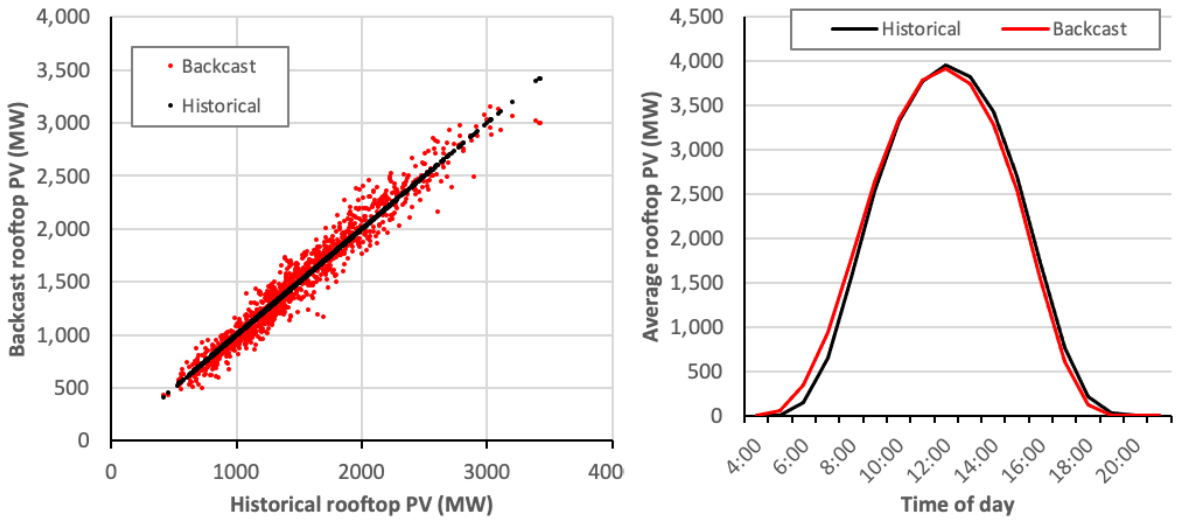

PV capacity growth is likely to occur through uptake by new dwellings and larger systems on existing dwellings. Some SEDs have had significantly higher uptake of rooftop PV than

[10] Australian PV Institute (APVI) Solar Map, funded by the Australian Renewable Energy Agency, accessed from pv-map.apvi.org.au

others as a percentage of dwellings; simply scaling all SEDs equally would not capture the likely greater geographical diversity in the future as the cost of installation continues to fall. Conversely, there may be genuine barriers to uptake in some areas. Therefore, uptake in each SED was first increased to halfway between its current level and the maximum density of all SEDs (59.9% of dwellings). Then capacity in all SEDs were scaled up to meet a target future megawatt capacity for each region.

3.5 Scenario definition

Two scenarios were modelled. The *Existing fleet* scenario models all existing wind, solar and rooftop PV capacity where a full year of data exists for at least calendar year 2021, with site specific calibration for wind farms.

The *Future NEM* scenario includes significantly more and varied renewable projects based on AEMO modelling of a near-zero-emissions 2050 scenario[11]. Representative traces for 54 wind and 47 solar locations across the mainland NEM[12] were simulated and scaled based on AEMO modelling for each Renewable Energy Zone. This scenario includes 62 GW of wind and 65 GW-ac of solar. 52 GW of rooftop PV across 104 distinct MERRA-2 grid points was also simulated. To be clear, this scenario represents only one possible view of the future, and actual build out will depend highly on optimising resource quality, diversity trade-offs, and transmission capacity.

4. Results

4.1 Instantaneous production

Figure 10 shows the generation-duration curve for as capacity factor (% of nameplate capacity) for both the *Existing fleet*, and the *Future NEM* fleet. The lowest backcast output for the existing fleet was a 0.59% capacity factor, at 4am 19th April 2020. This was confirmed by examining historical metered data for units that were installed by 2020, where the instantaneous production from mainland NEM utility VRE and rooftop PV fleet around that time fell as low as 0.31%[13]. For the future NEM fleet, the minimum fleet output is slightly higher (1.39% at 5pm 17th May 2010), consistent with the greater geographical diversity of capacity in that scenario.

[11] AEMO Draft Integrated System Plan Step-Change Scenario, available at https://aemo.com.au/-/media/files/major-publications/isp/2022/draft-2022-integrated-system-plan.pdf

[12] Tasmania was not included in the modelling, due to comparatively low interconnection and significant hydro fleet that would be utilised for storage in a high-VRE future.

[13] This occurred at 5:20am, slightly later than the simulated backcast, but all periods were low.

Figure 10 VRE capacity factor duration curve (relative to total fleet MW)

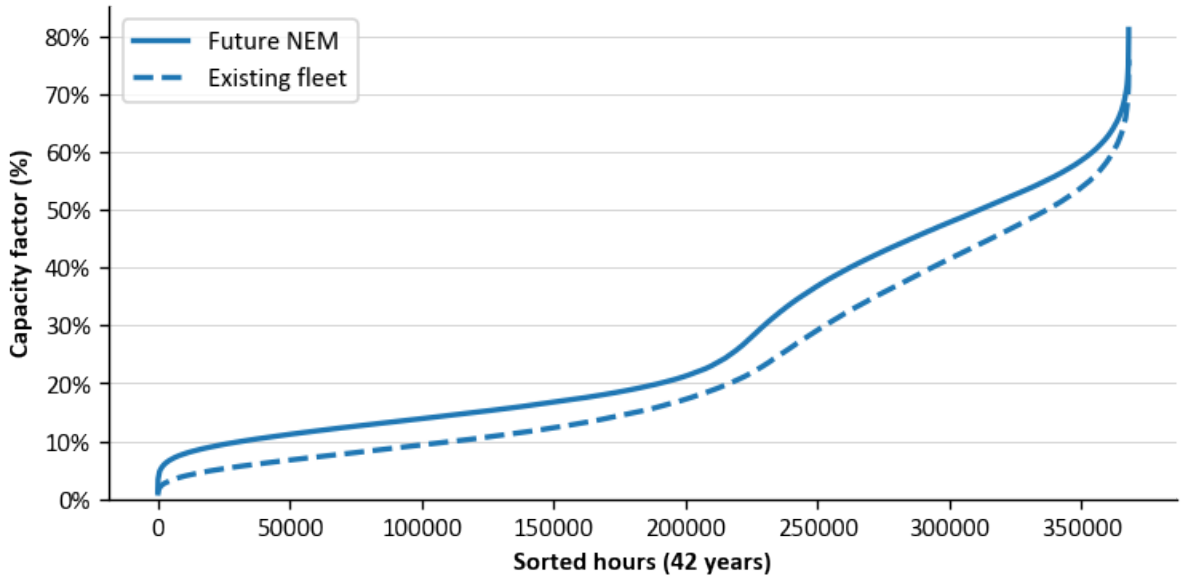

Figure 11 shows the week surrounding that period, which was driven by low wind production across the mainland NEM coinciding with the sun setting.

Figure 11 Future NEM output around worst hour (backcast 5pm 17th May 2010)

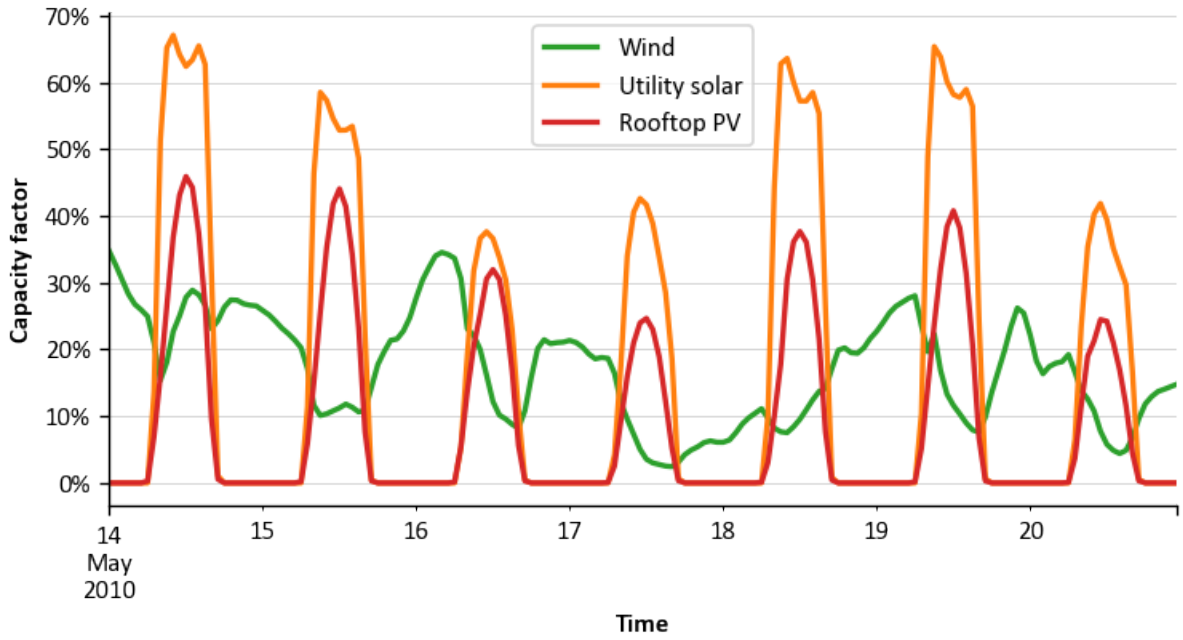

This shows that it is credible that a VRE fleet could deliver less than 1% of its nameplate in a small number of periods. These low periods may overlap with high demand mornings or

evenings, and sufficient firming capacity will be required. However, as Figure 12 shows, there is a strong diurnal trend of minimum VRE output over the dataset. Solar PV is significantly more predictable than wind: with a larger more geographically diverse future PV fleet (both utility and rooftop) the fleet's midday production can be relied upon for 25% of its capacity at a minimum, with the lowest VRE periods occurring overnight.

Figure 12 Backcast of lowest VRE outputs by time of day

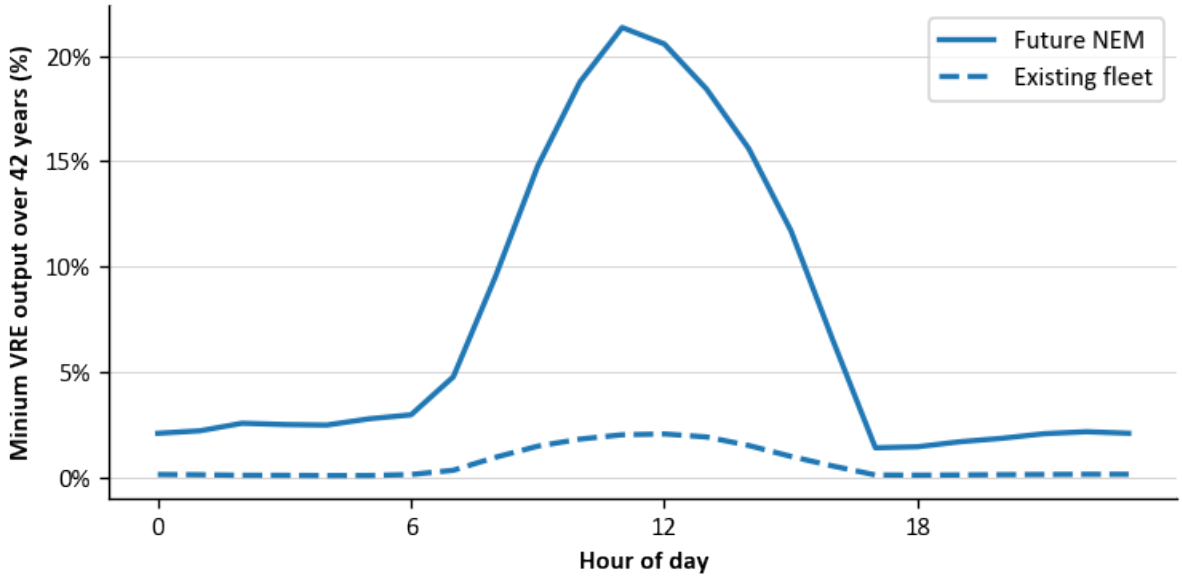

The specific quantity of instantaneous firming capacity will be dependent on the regional reliability standard and detailed modelling of the correlation between demand and wind. For example, in (Gilmore et al, 2022) simulations of a 100% renewable system yielded 25 GW of firming capacity against a peak demand of 30 GW. While the available VRE in that modelling was sometimes less than 1% of nameplate, these periods did not correspond with the peak demand periods. Conversely, during peak demand periods, the VRE fleet was more available. A question for policy makers will no doubt relate to whether it is preferable to procure the additional 5 GW of firming resources as insurance against low VRE production periods coinciding with peak demand.

Therefore, for the avoidance of doubt, this analysis does not suggest that the contribution to reliability of VRE projects is only 1% of its capacity[14]. Nevertheless, from a *planning* perspective, firming capacity comparable to the peak demand will likely be required.

[14] A proper assessment of firming value of VRE requires sophisticated modelling, such as Equivalent Load Carrying Capacity (ELCC).

4.2 VRE output over longer periods

Separate to the MW of capacity required, a key question is how much stored energy is needed to underpin firming capacity. A closely related question is the amount of renewable generation available over various timescales. Rather than comparing output to nameplate megawatts, we consider i) the energy available relative to the average production, which informs the daily and seasonal storage requirements, and ii) the energy relative to the "expected" seasonal output (defined below) which informs the magnitudes of renewable energy droughts (i.e., lower than expected output). Given the diurnal profile of solar and the likely availability of short-term storage in the future, we focus on the average output from the VRE fleet over one or more days.

Figure 13 shows the available energy over 1, 7, 14, and 28 days for each of the 42 simulated reference years, relative to the average generation over the entire study period. The blue line shows the average seasonal trend[15]. Outcomes for the *Existing fleet* scenario are similar, but with a smaller seasonal component due to the lower share of solar PV. To avoid repetition, we therefore focus on the *Future NEM* from this point.

Figure 13 Average VRE output over various timescales
(Future NEM, relative to 42-year mean; each thin series is one year, blue line is long-term average)

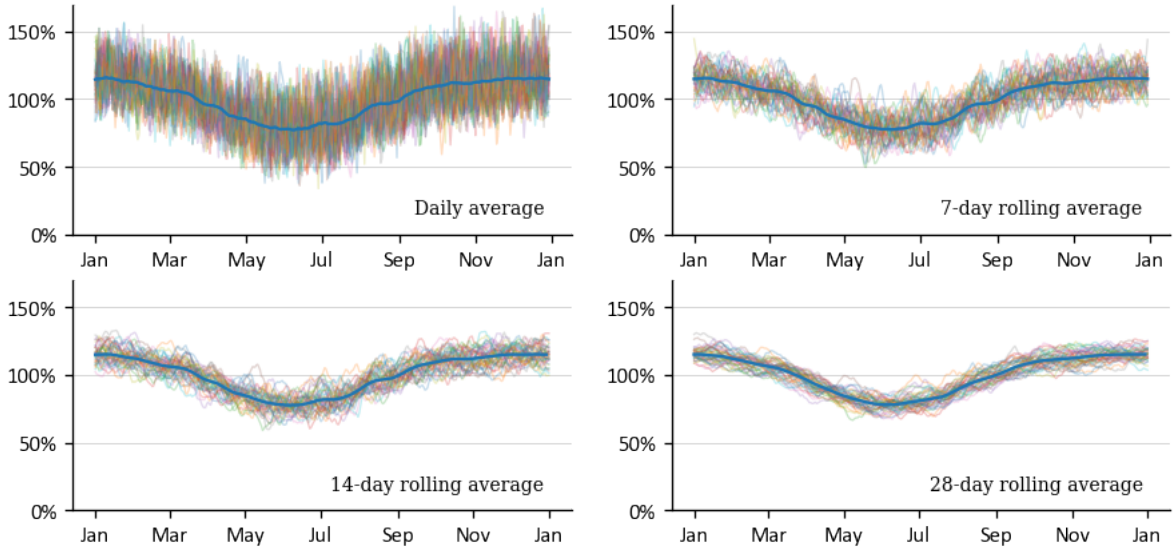

On the worst winter day, available energy falls to 32.6% of the long-term average, while the best days (typically October to December) exceed 150% of the long-term average. This

[15] The seasonal trend for daily output was defined as the centred, 14 day rolling mean output for that day across all 42 years. For example, the expected output for January 14th was defined as the mean output from January 7th to 21st from 1980 to 2021. For expected output over longer durations, these expected daily outputs were averaged (e.g., over 7 days) the same as the other reference year traces.

variability is a combination of seasonal trends (blue line) and daily weather variability, which is considered further in Section 4.3.

Critically, the variability reduces over longer timescales. Figure 14 shows the minimum output observed over 1 to 60 days (rolling average) for the VRE fleet (solid blue line) relative to the long-term mean. The worst 7 day period still delivers half (48.4%) of expected energy and the worst month two-thirds (64.7%). For any given renewable energy scenario, this approach can therefore quantify the spread of seasonal and daily outcomes.

The dotted lines in Figure 14 show the contribution from individual technologies. For shorter periods, the aggregate portfolio has a higher reliability of supply than any single technology – there is diversity of resource that helps avoid the worst periods. The worst (backcast) performance rapidly asymptotes for periods beyond three weeks[16]. Restricting the analysis to just the most recent 10 years of data underestimates the depth of the worst droughts over periods of up to seven days by ~10 percentage points and by ~5 percentage points over longer periods, with no single historical year being responsible for all worst-case events of all durations.

Figure 14 Lowest VRE output over various timescales (Future NEM, relative to 42-year mean)

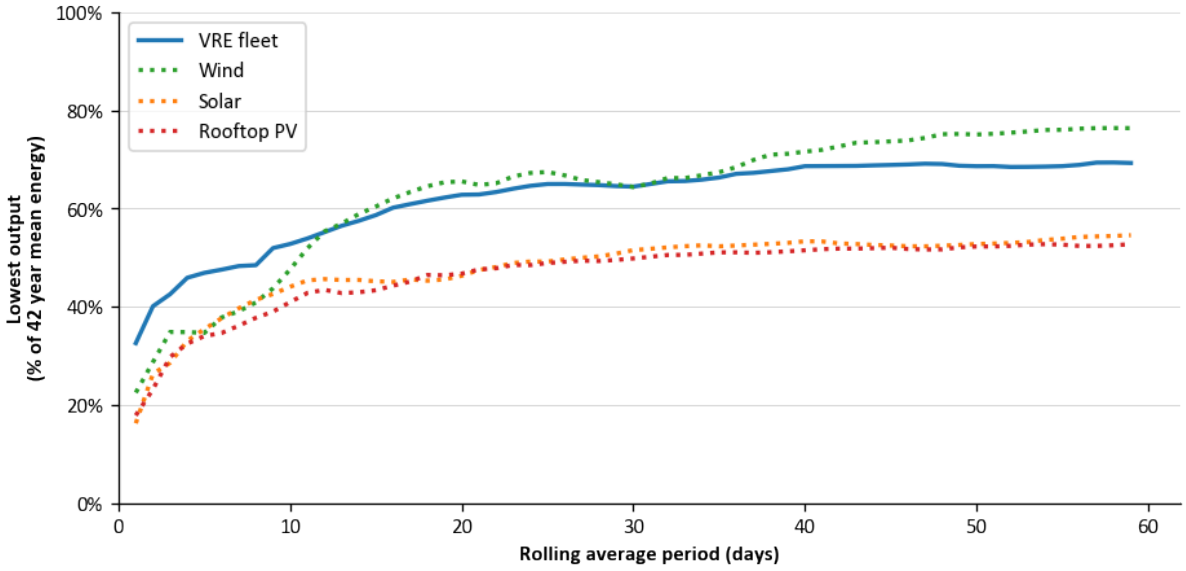

[16] By definition, the "worst" observed period gradually rises to the mean output (i.e., 100%) over enough periods, which is not shown on this figure.

4.3 Quantifying the risk of VRE droughts

Much of the variability described above would be anticipated by planners and investors. For example, the central blue line in Figure 13 highlights the strong seasonal trends in the simulated solar PV production. Suitable seasonal storage or other firming would naturally be developed given its predictability, and informed by the analysis of Section 4.2. However, policy makers will also be concerned about the inherent uncertainty of weather and hence of extended periods of low output (or "renewable droughts") not foreseen by planners.

It will therefore be helpful to separately quantify the *variability* of VRE output relative to *expected* or predictable trends in production[17]. Figure 13 shows, on any given day, available energy (coloured lines) varies by approximately 50% of the expected seasonal output (solid blue line). Over 7 days, this uncertainty reduces to ~30%, and over 28 days to ~20%. Once seasonal trends are taken into account, the "worst case" periods are milder. For example, historically over a two week period the available VRE energy does not fall below 75% of expected production. This is shown in Figure 15 which compares the absolute lowest output of renewables (the blue line from Figure 14) with the lowest output relative to the seasonal expected output (dashed black line).

Figure 15 Lowest VRE output versus expected output (long-term average or seasonal; Future NEM)

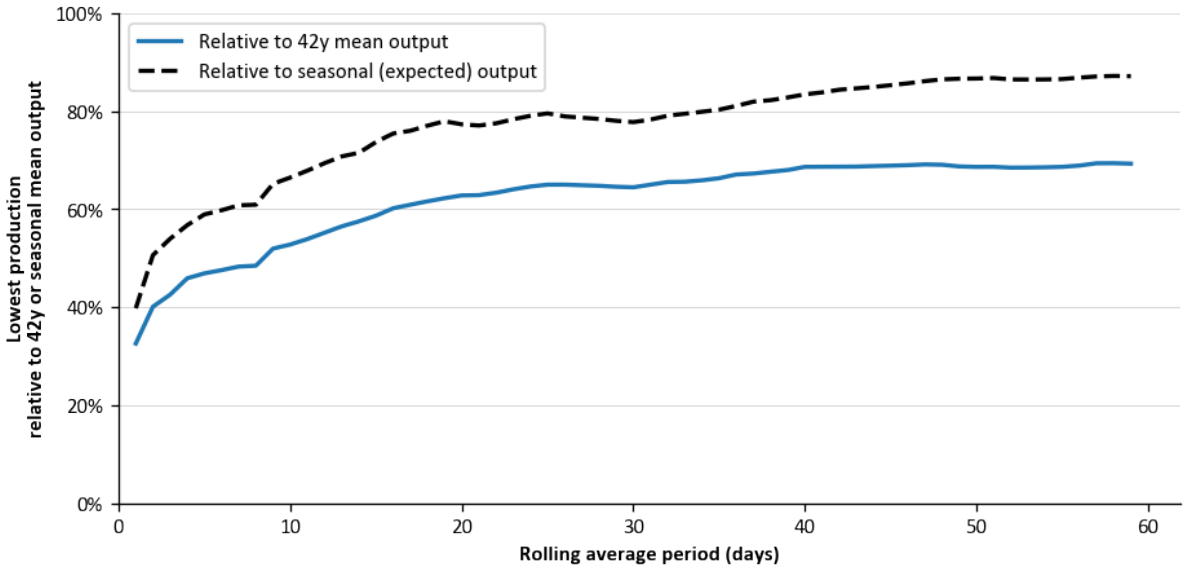

A key question is whether the worst case outcomes identified in Section 4.2 coincide with consumers' willingness to pay. Historically, reliability standards and market price caps have been used to avoid overbuilding capacity to cover very unlikely events. It is therefore

[17] The intra-day analogy is the diurnal profile of solar PV: this profile (particularly the lack of overnight solar energy) is well known and can be accounted for, while the variability of midday January output is a separate but important consideration.

necessary to quantify both the magnitude and frequency of renewable droughts. We adapt the Mean Below Threshold metric of Ohlendorf and Schill (2020) to measure consecutive days where the moving average capacity factor was below a particular threshold relative to the expected seasonal output[18]. The predictable seasonal variations (for instance, output in winter typically regularly being below 80% of the mean) are therefore netted out. The longest events were counted first, those periods removed from the data series, and then iteratively shorter periods counted (ensuring no overlapping events). The total number of events of a given duration or longer were then counted. The return period is then defined as the reciprocal of the average (mean) annual frequency of events of a given duration or longer.

Figure 16 shows the mean return period (average time between events) for average output being less than 85% and 70% of expected production. System planners therefore can have confidence that, relative to *expected* output, a "one in ten year" event is VRE output less than 70% of expected output for ten days, or less than 85% for 45 days. A one in 40 year event would be two weeks with output less than 70% of expected. There may be some long-tail events that are not captured in the 42 year sample period, but by definition these will be uncommon and therefore comparable with other non-credible events that are unlikely to be cost effective to plan against.

Figure 16 Average return period for VRE droughts (higher number means less frequent)

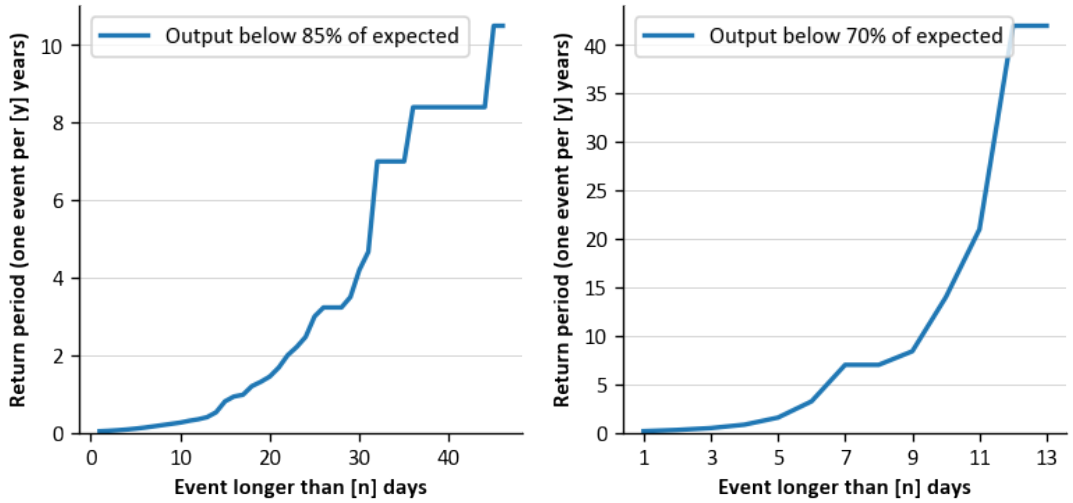

[18] Expected output was defined as the centred, 14 day rolling mean output across all 42 years. For example, the expected output for January 14th was defined as the mean output from January 7th to 21st from 1980 to 2021.

4.4 Solar tracking and winter risks

The main seasonal trends in Figure 13 are primarily driven by variability in solar output[19], which in turn is driven by two key assumptions. Firstly, all future solar PV systems are modelled with an AC/DC MW ratio of 1.2 (existing NEM sites typically have ratios between 1.05 and 1.33). Higher ratios will allow for more production during winter months with low insolation (with lesser impact on summer months), reducing annual variability. Secondly, all sites are assumed to be single-axis tracking, aligned north-south, consistent with the majority of announced projects. However, at lower latitudes of Australia, single axis tracking (SAT) sites perform particularly poorly over winter. This is because when the sun is low in the sky, the angle of incidence is unfavourable – particularly in the middle of the day. Conversely, fixed flat plate (FFP) systems, facing north with an elevation equal to their latitude, typically perform better. For example in Figure 17, Colleambally and Numurkah solar farms (SAT) have only a third to a half of the production over winter as they do in summer, while White Rock and Nyngan (FFP) see reductions of only ~20%.

Figure 17 Comparison of typical SAT (left) and FFP (right) average weekly solar production historical (black) and backcast (red) for Cal20

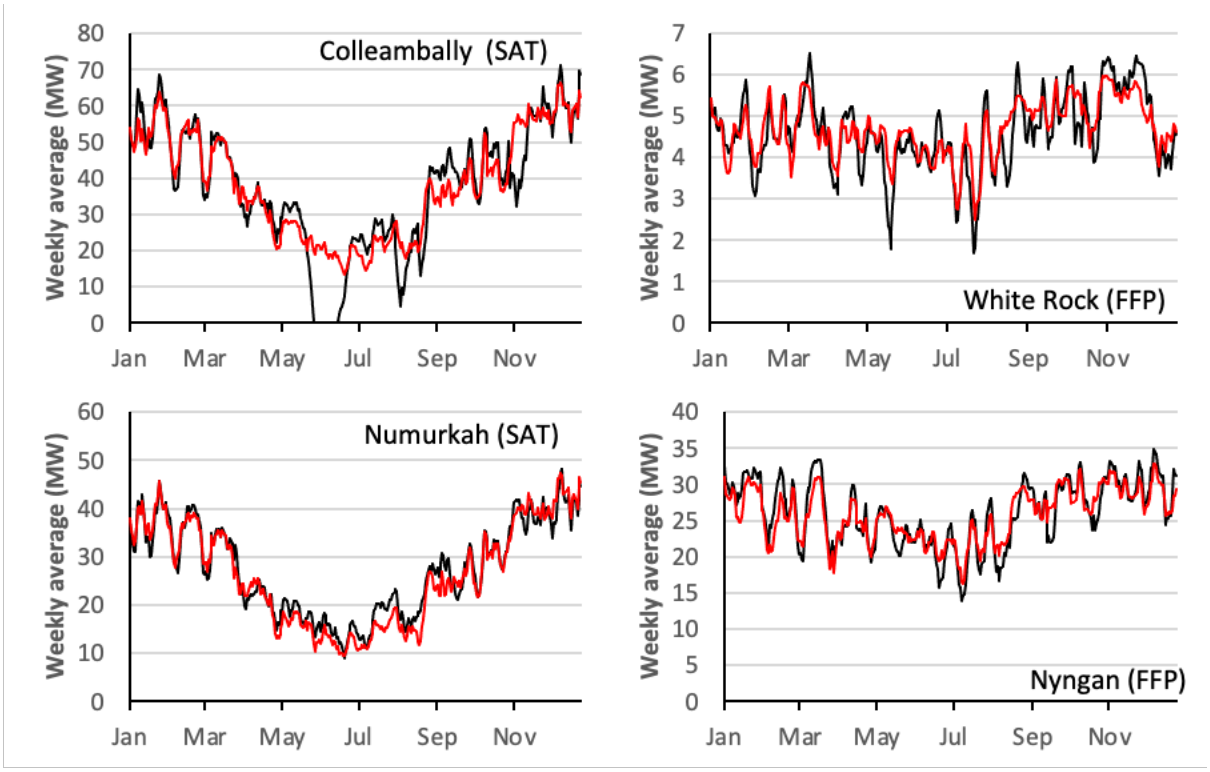

[19] Wind output is fairly constant across the year, slightly higher over the winter period (July-October) and lower in Autumn.

In a future high VRE penetration grid, it may therefore be beneficial to include some FFP solar, particularly in the southern states. If all utility solar was FFP instead of SAT, roughly 7% more energy could be delivered over the winter months (Figure 18), reducing the need for seasonal firming. As shown in Figure 19, this would reduce the worst observed VRE events by roughly 3-8 percentage points. This additional winter production generally comes at the expense of some net annual production (roughly 2% given the assumptions of this modelling) but avoids the cost of the tracking system; on balance, studies typically find a slightly lower levelized ($/MWh) cost for SAT solar[20], but this cost may be small compared to the resulting seasonal firming benefits. As energy policy evolves, it will be important for policy makers to consider that energy production value will vary not just intra-day but across the year as well.

Figure 18 Change in seasonal output from switching from SAT solar to FFP solar

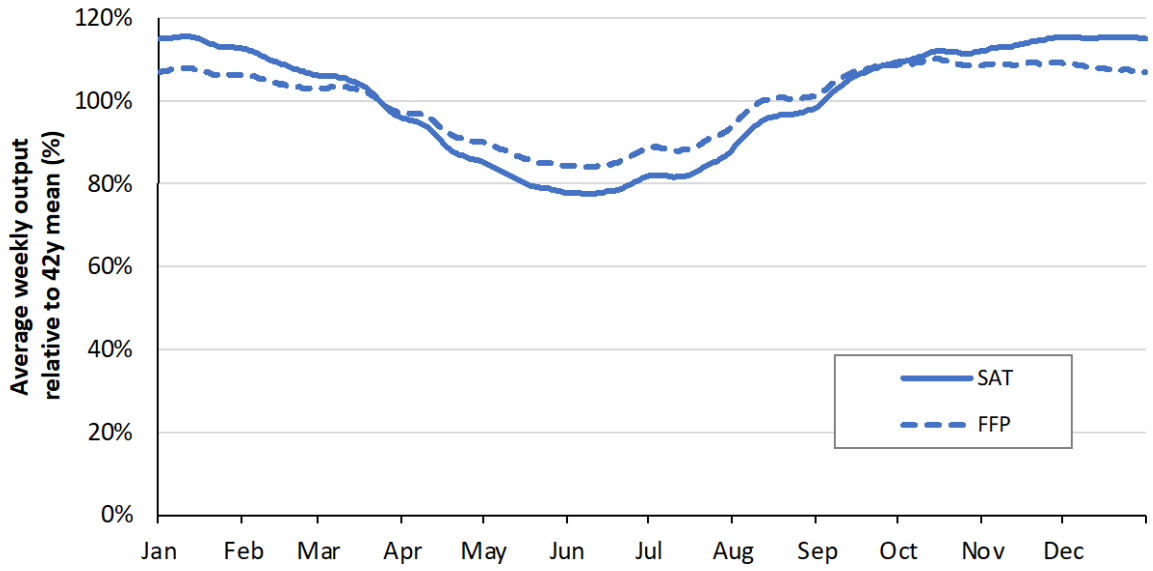

[20] For example, https://www.nrel.gov/pv/lcoe-calculator/

Figure 19 Worst VRE periods with single-axis and fixed plate solar (Future NEM, relative to 42-year mean)

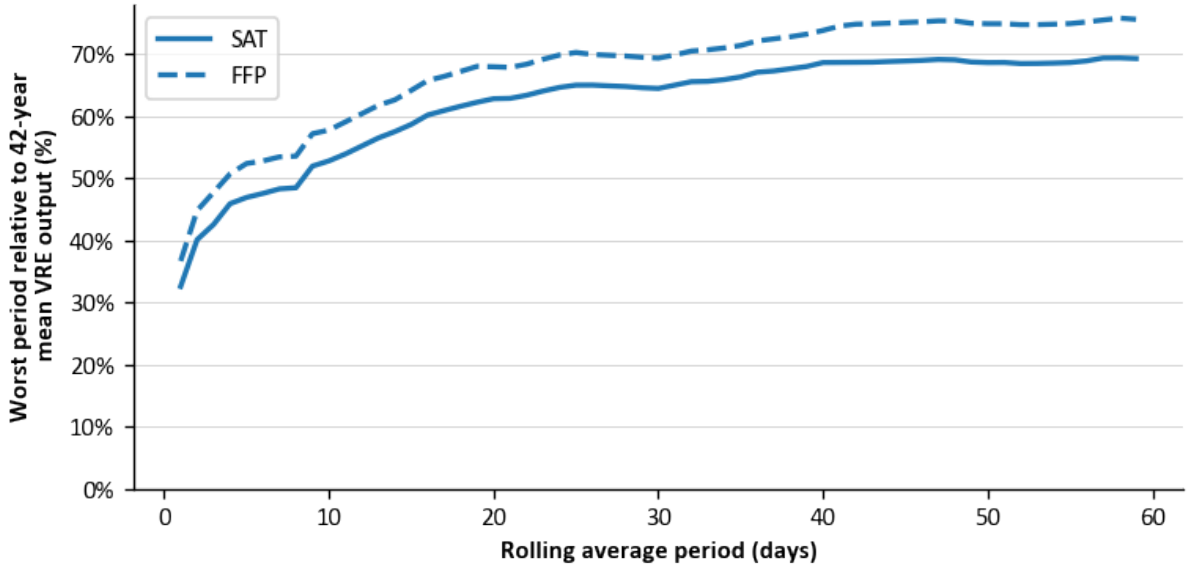

4.5 Benefit of geographical diversity

Strong interconnection between regions will have a benefit in reducing the risk of prolonged outages. Figure 20 shows similar analysis to Figure 14 on a regional level (dotted lines) and then for the combined fleet (for the Future NEM portfolio). This shows that each state, on its own, would have lower possible VRE performance compared to the NEM-wide output, when evaluated over (between) 1 and 10 days. While regions will no doubt have their own dedicated firming resources (both to ensure local needs are met and to manage potential interconnector outages) this suggests that strong interconnection will materially reduce the risk of energy shortfalls. The benefit of reduced firming requirements may not be considered in transmission planning studies (such as the ISP and associated RIT-T calculations) if sufficient resource variability (i.e., reference years) have not been considered.

Figure 20 Worst periods in individual states and the fleet (Future NEM, relative to 42-year mean)

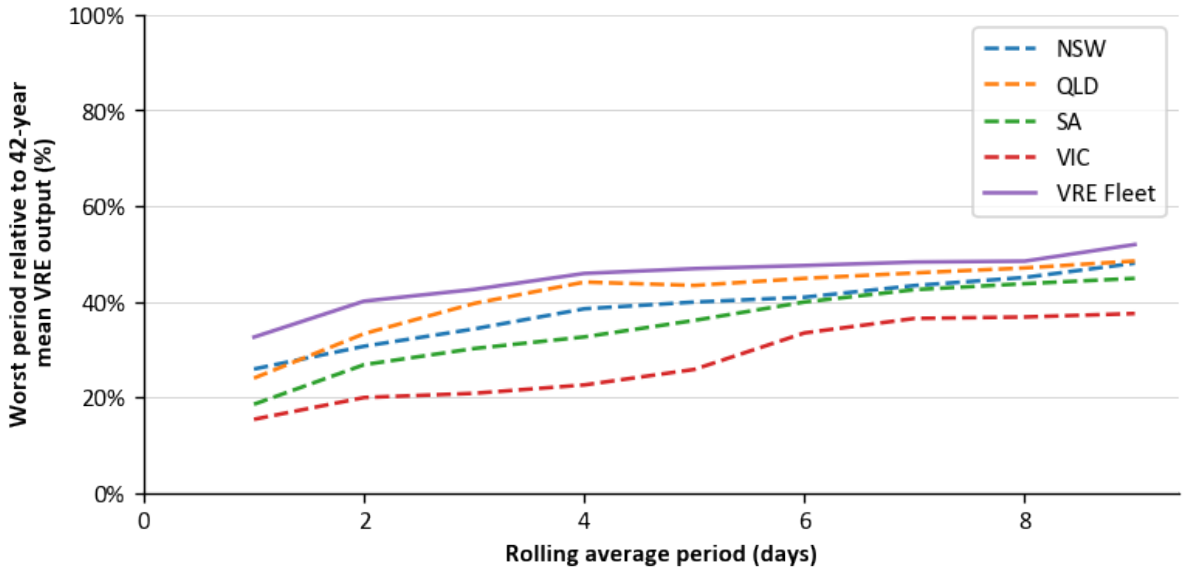

4.6 Ramping requirements in the NEM

This modelling can also be used to consider the future maximum ramping requirement in the NEM, shown in Figure 21. On the worst days, available production can shift by over 40 GW in an hour (out of installed VRE capacity of 180 GW). This is primarily driven by predictable changes in large-scale and rooftop solar production over morning and evening ramp ups, but hourly wind production changes of up to 15 GW (one quarter of the installed capacity) were also observed. In practice, this will be mitigated by either energy storage or curtailment during the highest output periods, but hourly changes of 20-30 GW will be common in the future grid and will require flexible generation and load. Policy makers will need to ensure that sufficient signals for flexibility (and, conversely, not overvaluing existing inflexible capacity) are available in the market. For example, capacity markets might need to further derate units based on their flexibility and ramping capability, requiring consideration of unit commitment strategies in any modelling.

Figure 21 Worst daily VRE ramp rates (MW change per hour in Future NEM scenario)

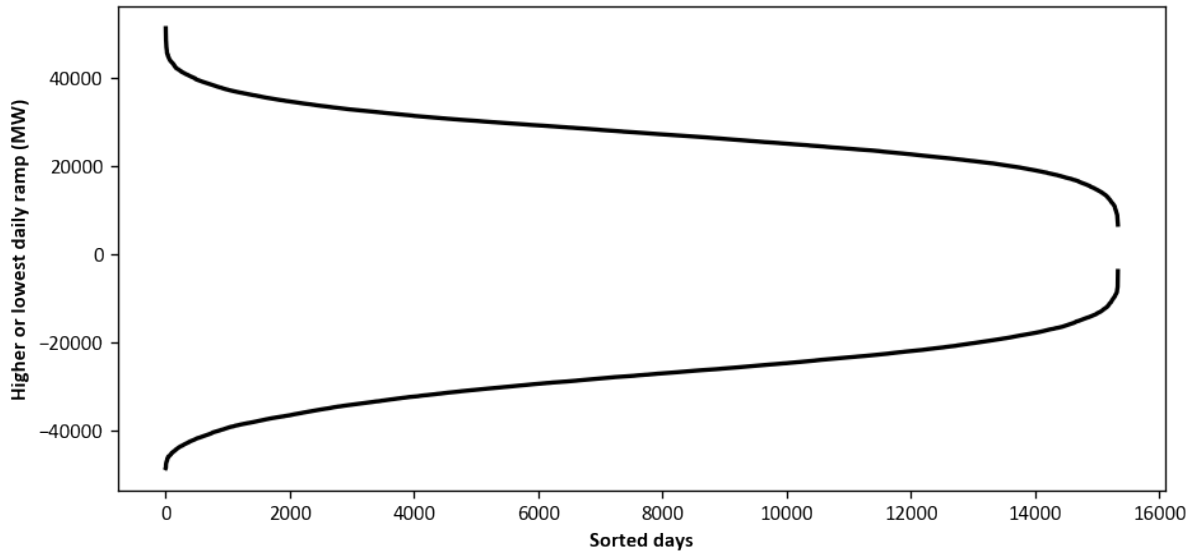

5. Discussion and conclusions

The NEM is rapidly transitioning to a ~100% VRE system, with the majority of energy supplied by weather dependent energy resources. Just as the NEM has historically had headroom of installed capacity above peak demand to allow for outages, it is likely that the future grid will have headroom around its available energy. This paper helps to quantify these future requirements.

Through the MERRA-2 reanalysis dataset, we have undertaken a calibrated backcast of the existing VRE fleet as well as a hypothetical Future NEM fleet with greater geographical distribution. While the concept of energy droughts have received much attention, we do not find evidence of extended time periods of low VRE production in the NEM. For example, over a two-week period in the worst historical time sequence, the VRE fleet would still have delivered 54% of its average output or 70% of the *expected* output once seasonal trends (e.g., winter solar production) are taken into account. A 30% reduction in expected energy is therefore the worst two-week historical VRE drought on record.

These figures also assume no curtailed energy. In practice, it will almost always be efficient to overbuild renewables at a local level (for example, to better utilise a costly transmission line). The market operator (in the AEMO ISP results that inform the *Future NEM* scenario) projects 20% VRE curtailment by 2050, while (Simshauser et al., 2021) have suggested that a 20% to 240% overbuild of capacity on a transmission line would be efficient. The subsequent curtailment will reduce variability of output and deliver more constant energy both daily and seasonally, reducing the risks of droughts.

Based on this analysis, the previous VRE drought risks may have been overstated. Indeed, the authors of this paper previously considered a "worst case" VRE drought sensitivity (Gilmore et al., 2022) where wind and solar production was capped at (or below) 10% of their respective nameplate capacities for a seven-day period. In that period, the fleet delivered only 18.9% of its average production compared to the worst-case 53.4% projected above. Longer but milder energy droughts were moderately underestimated, however.

Implications for planners and policy makers

This analysis is critical for investors, planners, and the system operator in considering the needs of the future grid. The variability in renewable output over various timescales can be used to enhance planning models. The optimal build of firming naturally requires more sophisticated modelling, but these figures can provide intuition to policy makers in three key areas.

Firstly, it highlights the amount of firming required. For example, consider the simplest case of flat demand across the year, and the VRE fleet were built such that average generation equalled average demand. Section 4.2 suggests the *worst case* firming energy requirements would be equal to i) two-thirds of the daily average energy demand; and ii) one-third of average monthly energy demand. This firming could be delivered through conventional hydro, seasonal energy storage, or zero emissions gas peaking units but "overbuilding" the renewable energy fleet (that is, allowing for some spilled energy over time) is also likely to be an efficient source of energy firming. The relatively flat production risk over periods longer than two weeks (Figure 15) means technologies that can deliver additional energy over longer periods will be favoured (i.e., building additional VRE capacity and fuel based technologies such as zero emission OCGTs). A highly flexible demand side (e.g., hydrogen export industry) will support additional VRE build and provide its own source of firming.

To deliver this firming, utilities with diverse portfolios will then incorporate firming strategies (including assuming VRE will only produce at a P70 (70th percentile) level) to manage both capacity and energy risks. Historically, it has been reasonable to expect that "1 in 10 year" risks can be managed[21]. However, this analysis (Section 4.3) shows that 1-in-20 or 1-in-40 year VRE droughts are possible, and it may not be prudent for private utilities to invest to cover these risks. Therefore, these periods would either require a suitably flexible demand side, or some additional energy reserves to be procured by governments on behalf of the community and energy users. This energy would need to be held in reserve out of the market, so as not to simply substitute for prudent utility hedging. As such, policy makers should urgently consider the investment timeframe capacity reserve suggested by Nelson et al (2022) and an operating reserve that could be utilised to deliver this outcome.

Secondly, this analysis highlights that traditional capacity markets, where compliance is measured through capacity availability, will almost certainly not provide the required signal for sufficient energy production. Instead, real-time scarcity signals will be critical for providing investors with the necessary signals (i.e., price exposure) to invest in long-duration firming

[21] More extreme conditions are then either managed through spot markets, reserve capacity schemes, or load shedding consistent with the relevant reliability standard.

technologies. The NEM's energy only market seems well suited to this purpose (Riesz et al., 2016), with a Market Price Cap of $15,500/MWh that imposes a strong penalty for not delivering on contracted positions. A key parameter is the Cumulative Price Threshold (CPT)[22] that caps spot prices at $300/MWh if average prices over a 7-day period exceed a threshold ($692/MWh). Increasing this trigger will provide a stronger incentive for utilities to invest in longer duration storage, in particular.

Finally, we find that diversity of resource between regions will help reduce the risk of localised droughts, and so governments should work quickly to strengthen regional interconnectors. The entire process of economic consideration of transmission investment requires an overhaul. Economic cost benefit analyses should include a longer-term timeframe analysis of resource variability as well as carbon constraints and budgets.

Concluding remarks

It is indeed physically and economically possible to power Australia's NEM using energy entirely sourced from variable energy-dependant resources supported by storage and firming technologies. To achieve Australia's emissions reduction commitments, it will be important for policy makers to embrace the transition and design incremental changes to the market framework to deliver this outcome.

6. References

Ebisuzaki, W., Zhang, L., 2014. Reanalyes, best practices, 12th climate prediction applications science workshop (CPASW).

Gelaro, R., McCarty, W., Suárez, M.J., Todling, R., Molod, A., Takacs, L., Randles, C.A., Darmenov, A., Bosilovich, M.G., Reichle, R., Wargan, K., Coy, L., Cullather, R., Draper, C., Akella, S., Buchard, V., Conaty, A., Da Silva, A.M., Gu, W., Kim, G.-K., Koster, R., Lucchesi, R., Merkova, D., Nielsen, J.E., Partyka, G., Pawson, S., Putman, W., Rienecker, M., Schubert, S.D., Sienkiewicz, M., Zhao, B., 2017. The Modern-Era Retrospective Analysis for Research and Applications, Version 2 (MERRA-2). Journal of Climate 30, 5419-5454.

Gilmore, J., Nelson, T., Nolan, T., 2022. Firming technologies to reach 100% renewable energy production in Australia's National Electricity Market (NEM). CAEEPR working paper, Griffith University.

Haas, S., Krien, U., Schachler, B., Bot, S., petrou, k., Zeli, V., Shivam, K., Bosch, S., 2021. windpowerlib—a python library to model wind power—v0.2.1.

[22] The CPT is intended to prevent systemic financial impacts on market participants under extreme conditions.

Hallgren, W., Gunturu, U.B., Schlosser, A., 2014. The potential wind power resource in Australia: A new perspective. PLoS ONE 9.

Holmgren, W.F., Hansen, C.W., Mikofski, M.A., 2018. pvlib python: a python package for modeling solar energy systems. Journal of Open Source Software 3, 884.

Katsigiannis, Y.A., Stavrakakis, G.S., 2014. Estimation of wind energy production in various sites in Australia for different wind turbine classes: A comparative technical and economic assessment. Renewable Energy 67, 230-236.

Kohler, S., Agricola, A.-C., Seidl, H., 2010. dena-Netzstudie II.Integration erneuerbarer Energien in die deutsche Stromversorgung im Zeitraum 2015 – 2020 mit Ausblick auf 2025.

Maxwell, E.L., 1987. A Quasi-Physical Model for Converting Hourly Global Horizontal to Direct Normal Insolation.

McPherson, M., Karney, B., 2017. A scenario based approach to designing electricity grids with high variable renewable energy penetrations in Ontario, Canada: Development and application of the SILVER model. Energy 138, 185-196.

McPherson, M., Sotiropoulos-Michalakakos, T., Harvey, L.D.D., Karney, B., 2017. An Open-Access Web-Based Tool to Access Global, Hourly Wind and Solar PV Generation Time-Series Derived from the MERRA Reanalysis Dataset. Energies 10, 1007.

Meinshausen, M., Lewis, J., McGlade, C., Gütschow, J., Nicholls, Z., Burdon, R., Cozzi, L., Hackmann, B., 2022. Realization of Paris Agreement pledges may limit warming just below 2 °C. Nature 604, 304-309.

Nelson, T., Nolan, T., Gilmore, J., 2022. What's next for the Renewable Energy Target – resolving Australia's integration of energy and climate change policy? Australian Journal of Agricultural and Resource Economics 66, 136-163.

Nørgaard, P., Holttinen, H., 2004. A Multi-Turbine Power Curve Approach.

Ofgem, 2012. Electricity Capacity Assessment.

Ohlendorf, N., Schill, W.-P., 2020. Frequency and duration of low-wind-power events in Germany. Environ. Res. Lett. 15.

Olauson, J., Bergkvist, M., 2016. Correlation between wind power generation in the European countries. Energy 114, 663-670.

Pfenninger, S., Staffell, I., 2016. Long-term patterns of European PV output using 30 years of validated hourly reanalysis and satellite data. Energy 114, 1251-1265.

Poletti, S., Staffell, I., 2021. Understanding New Zealand's wind resources as a route to 100% renewable electricity. Renewable Energy 170, 449-461.

Prasad, A.A., Taylor, R.A., Kay, M., 2017. Assessment of solar and wind resource synergy in Australia. Applied Energy 190, 354-367.

Riesz, J., Gilmore, J., MacGill, I., 2016. Assessing the viability of energy-only markets with 100% renewables: An Australian National Electricity Market case study. Economics of Energy & Environmental Policy 5, 105-130.

Santos, J.A., Rochinha, C., Liberato, M.L.R., Reyers, M., Pinto, J.G., 2015. Projected changes in wind energy potentials over Iberia. Renewable Energy 75, 68-80.

Simshauser, P., Billimoria, F., Rogers, C., 2021. Optimising VRE Plant Capacity in Renewable Energy Zones. Faculty of Economics, University of Cambridge.

Sinden, G., 2007. Characteristics of the UK wind resource: Long-term patterns and relationship to electricity demand. Energy Policy 35, 112-127.

Staffell, I., Green, R., 2014. How does wind farm performance decline with age? Renewable Energy 66, 775-786.

Staffell, I., Pfenninger, S., 2016. Using bias-corrected reanalysis to simulate current and future wind power output. Energy 114, 1224-1239.

Tong, D., Farnham, D.J., Duan, L., Zhang, Q., Lewis, N.S., Caldeira, K., Davis, S.J., 2021. Geophysical constraints on the reliability of solar and wind power worldwide. Nature Communications 12.

Wang, C., Dargaville, R., Jeppesen, M., 2018. Power system decarbonisation with Global Energy Interconnection – a case study on the economic viability of international transmission network in Australasia. Global Energy Interconnection 1, 507-519.

Wild, M., Folini, D., Henschel, F., Fischer, N., Müller, B., 2015. Projections of long-term changes in solar radiation based on CMIP5 climate models and their influence on energy yields of photovoltaic systems. Solar Energy 116, 12-24.

William, Z., Martin, J., Machteld van den, B., 2019. Is a 100% renewable European power system feasible by 2050? Applied Energy 233-234, 1027-1050.